Saudi Pharmaceutical Journal 29 (2021) 963–975

Contents lists available at ScienceDirect

Saudi Pharmaceutical Journal

journal homepage: www.sciencedirect.com

Original article

Preparation, characterization, dissolution, and permeation of flibanserin – 2-HP-β-cyclodextrin inclusion complexes

Adel F. Alghaith [a], Gamal M. Mahrous [a,*], Diaa Eldin Zidan [a], Nabil A. Alhakamy [b], Abdulmohsin J. Alamoudi [c], Awwad A. Radwan [d]

[a] Department of Pharmaceutics, College of Pharmacy, King Saud University, PO Box 2457, Riyadh 11451, Saudi Arabia
[b] Department of Pharmaceutics, Faculty of Pharmacy, King Abdulaziz University, Jeddah, Saudi Arabia
[c] Department of Pharmacology and Toxicology, Faculty of Pharmacy, King Abdulaziz University, Jeddah, Saudi Arabia
[d] Kayyali Chair, College of Pharmacy, King Saud University, Saudi Arabia

ARTICLE INFO

Article history:
Received 30 March 2021
Accepted 16 July 2021
Available online 21 July 2021

Keywords:
Hydroxypropyl-β-cyclodextrin (HP-β-CD)
Sodium lauryl sulfate (SLS)
Flibanserin (FLB)
Solubility
Dissolution
Permeation

ABSTRACT

Flibanserin (FLB), an antiserotonin drug, is used to treat women with hypoactive sexual appetite disorder. FLB shows low bioavailability (~33%) probably due to its low water solubility. The current study investigated the impact of hydroxypropyl-β-cyclodextrin (HP-β-CD) and sodium lauryl sulfate (SLS) on the dissolution and permeation of FLB. HP-β-CD–FLB inclusion complexes were prepared using physical mixing and kneading at 1:1 and 1:2 M ratios and characterized using differential scanning calorimetry, Fourier transform infrared spectroscopy, and powder X-ray diffractometry. The dissolution and permeation of the complexes through a cellophane membrane were performed in, 0.1, 0.3 and 0.5% SLS in phosphate buffer (pH 6.8).

Derived from the slope of the linear phase solubility diagram, the apparent stability constant ($K_{1:1}$) was 372.54 M^{-1}. Kneading changed the crystalline form of FLB to an amorphous appearance characterized by minimal crystalline peaks, indicating successful inclusion complex formation. In addition, the HP-β-CD–FLB inclusion complexes showed twofold increased dissolution efficiency at 6 h. The cumulative FLB amount permeated at 6 h increased from 14.1% to 21.88% and 34.56% in the presence of 0.1% and 0.3% of SLS, respectively. However, increasing SLS to 0.5% did not show an increase in FLB permeation. Therefore, the HP-β-CD–FLB inclusion complex has an improved dissolution rate compared to FLB alone. The presence of SLS in the dissolution medium increases the dissolution rate of pure FLB and its complex with HP-β-CD. kneaded 1:1 complex was formulated bioadhesive buccal tablets and showed enhanced drug release.

1. Introduction

Flibanserin (FLB; $C_{20}H_{21}F_3N_4O$) is a nonhormonal drug used to treat women with hypoactive sexual appetite disorder. The mechanism of action of FLB in maintaining a healthy sexual response is based on decreasing serotonin and increasing norepinephrine and dopamine levels (Allers et al., 2010; Invernizzi et al., 2003). Compared with a placebo, 100 mg of FLB was shown to improve the overall score of the female sexual function index and the number of sexual events (Katz et al., 2013). However, FLB has low bioavailability (~33%), which might be attributed to its poor water solubility and extensive first-pass metabolism (CYP3A4 and CYP2C1), producing inactive metabolites (English et al., 2017; Fahmy et al., 2020). This poor water solubility of FLB is a limiting factor for its dissolution in body fluids and absorption via mucosal membranes.

Cyclodextrins (CDs) are a family of compounds widely used to increase the solubility of poorly water-soluble compounds by forming inclusion complexes (Raj et al., 2016). CDs are cyclic oligosaccharides are derived from starch and are composed of α-(1 → 4)-linked α-d-glucopyranose. These cyclic oligosaccharides contain a hydrophilic shell and a central hydrophobic core (Malaekeh-Nikouei et al., 2007). Complexes with different compounds are formed by the inclusion of hydrophobic drugs into

* Corresponding author.
E-mail address: gmmarous@ksu.edu.sa (G.M. Mahrous).
Peer review under responsibility of King Saud University.

Production and hosting by Elsevier

https://doi.org/10.1016/j.jsps.2021.07.019
1319-0164/

the central hydrophobic cavity of these compounds. Inclusion complexes have many advantages, such as enhanced solubility, bioavailability, and stability. Furthermore, they are beneficial in masking bad tastes or odors and in transforming gases or liquids into solid forms (George and Vasudevan, 2012). CDs are classified on the basis of the number of glucose molecules present in their backbone into α-CD (6-glucopyranose units), β-CD (seven glucopyranose units), and γ-CD (eight glucopyranose units) (Vikas et al., 2018). Different CDs show different cavity sizes due to the variation in the number of glucopyranose units and hence show different physical characteristics; for example, β-CDs have low solubility. Therefore, modified β-CDs, including hydroxypropyl-beta-cyclodextrin (HP-β-CD, formed by the addition of propylene oxides to several hydroxyl groups of a β-CD), have been developed to enhance the aqueous solubility and safety profiles of parent β-CDs (Carrier et al., 2007).

Improving the dissolution rate and hence the solubility of hydrophobic (class II) drugs is essential for increasing their oral bioavailability (Qiang et al., 2010; Rasenack and Muller, 2005). A widely adopted strategy to improve both the dissolution rate and the solubility of hydrophobic drugs is to incorporate the anionic surfactant sodium lauryl sulfate (SLS) into the formulation. SLS, a high solubilizing potential surfactant, can improve drug solubility by forming micelles that encapsulate various poorly soluble drugs into their hydrophobic core of these micelles. This work aims to evaluate the impact of combining HP-β-CD and SLS on the dissolution and permeation of FLB to overcome its solubility and bioavailability issues. HP-β-CD–FLB inclusion complexes were formulated using kneading in 1:1 and 1:2 M ratios. In addition, the prepared complexes were characterized using differential scanning calorimetry (DSC), Thermogravimetric analysis(TGA), powder X-ray diffractometry (XRD), and Fourier transform infrared spectroscopy (FTIR). The dissolution and permeation through a cellophane membrane of the prepared complexes were performed in 0.0%–0.5% SLS in phosphate buffer (pH 6.8) to study the effects of HP-β-CD and SLS on the dissolution and permeation of FLB. Furthermore, kneaded 1:1 complex was formulated bioadhesive buccal tablets and evaluated for drug release.

2. Materials and methods

2.1. Materials

FLB was purchased from Qingdao Sigma Chemical Co., Ltd. (Qingdao, China). SLS from BDH Co. (Poole, England). HP-β-CD from Signet Chemical Corporation Pvt. Microcrystalline cellulose (MCC) and Carpobol 934 were obtained from Serva GmbH Co (Heidelberg, Germany). Other chemicals were of analytical grade and were used without further purification. The dialyzing cellophane membrane (molecular weight cutoff 8000) was acquired from Spectrum Medical Inc. (Los Angeles, CA, USA).

2.2. Methods

2.2.1. Spectrophotometric scanning of FLB

To identify the wavelength of maximum absorption (λ_{max}), FLB at a defined concentration in phosphate buffer (pH 3.0) was spectrophotometrically scanned at 200–400 nm. UV spectrophotometric scanning of FLB solutions was also performed in the presence of HP-β-CD and the surfactant at the same wavelength intervals.

2.2.2. Construction of FLB calibration curve

FLB concentrations were determined spectrophotometrically at λ_{max} = 244 nm. To construct an FLB calibration curve, 10 mg of the drug was accurately weighed and dissolved in 100 mL of 0.01 N HCl. In McIlvian phosphate buffer (pH 6.8), serial dilutions were prepared to obtain different concentrations (25, 50, 75, 100, 150, 200, and 400 μg/mL) of the drug. The solvent medium was also used as a blank. The mean of three readings was plotted as a function of concentration.

2.2.3. Phase solubility studies

Excess FLB (50 mg) was mixed with 5 mL of distilled water in closed stoppered test tubes containing different HP-β-CD concentrations (25–100 mM), as described by Higuchi and Connors (1965). After shaking for 48 h at 37 °C ± 1 °C in a shaking water bath to reach equilibrium, samples were collected in triplicate and subsequently filtered through a 0.45 μm polyvinylidene difluoride (PVDF) membrane filter. Diluted samples were analyzed using a UV-1700 UV spectrophotometer (Shimadzu, Japan) at a wavelength of 244 nm against CD-in-water blanks with identical concentrations. The mean of three readings was recorded. The apparent stability constant (K_c) of the complexes prepared at a 1:1 stoichiometric ratio was calculated from the phase solubility diagrams using the following equation:

$$K_c(1:1) = \text{Slope}/S_o(1 - \text{slope}) \quad (1)$$

The initial straight-line portion of the FLB concentration–HP-β-CD plot was used to obtain the slope, and S_o (the equilibrium solubility of FLB in water without HP-β-CD).

In addition, complexation efficiency (CE) was calculated using the following equation: (Loftsson et al., 2005).

$$CE = \text{Slope}/1 - \text{slope} \quad (2)$$

2.2.4. Preparation of solid inclusion complexes

The following inclusion complexes of FLB and HP-β-CD were formulated at molar ratios of 1:1 and 1:2:

2.2.4.1. Physical mixture. FLB and HP-β-CD at 1:1 &1:2 M ratios were formulated into a physical mixture by mixing these components that have been sieved previously through sieve no 60.

2.2.4.2. Kneading method. During a 1 h of trituration, FLB and HP-β-CD at a molar ratio of 1:1&1:2 were wetted with acetone to form a kneaded-like paste and was ground in a mortar resulting in the evaporation of the solvent. The obtained kneading mass was then dried for 48 h and pulverized, resulting in the formation of a powder-like complex.

2.2.5. Differential scanning calorimetry and thermogravimetric analysis

DSC was used to study the interplay between the CD and the drug molecules. DSC was performed on FLB, HP-β-CD, their physical mixtures, and the 1:1 HP-β-CD–FLB inclusion complex using Perkin Elmer DSC8000 (USA). Briefly, 5–7 mg samples were put into aluminum pans and sealed. In the DSC runs, the heating rate was set to 5 °C/min over 25 °C–300 °C. Software analysis was conducted for every sample to determine the peak temperature, heat of fusion, and glassy transitions.

TGA of FLB, HP-β-CD, their physical mixtures, and the 1:1 HP-β-CD–FLB inclusion complex was performed using Perkin Elmer TGA analyzer. A sample of about 3 mg was placed in a flat-bottomed aluminum pan and heated with the range from 30 °C to 800 °C by the rate of 10 °C min-1 in dry nitrogen stream.

2.2.6. Fourier transform infrared spectroscopy

The FT/IR-4100 type A machine was used to record the FTIR spectra of FLB, HP-β-CD, their physical mixtures, and the 1:1 HP-β-CD–FLB inclusion complex. A KBr disc was used to prepare sam-

ples; 2 mg of the sample was combined with 200 mg of KBr. The scanning range was from 400 to 4000 cm^{-1}.

2.2.7. Powder X-ray diffractometry

XRD patterns of the powdered sample and the crystallinity of pure FLB and its complexes were determined using a RIGAKU diffractometer (Japan) fitted with a curved monochromatic graphite crystal, an automatic divergence slit, and a PW/1710 automatic controller. The target used was CuK-based radiation operating at 40 KV and 40 mA (~1.5418 Å). The XRD patterns were obtained via continuous-mode scanning from 4° to 140° with 2° variation.

2.2.8. Preparation of buccal bioadhesive FLB tablets

Bioadhesive tablet formulations of FLB using the 1:1 HP-β-CD–FLB kneaded inclusion complex 1:1 with a drug equivalent to 25 mg were prepared. The components of each formula, as described in Table 1, were mixed for 15 min in a Turbula mixer (Type S27; Erweka, Germany). The formulations were compressed into tablets using 9.5 mm flat punches in a single punch tablet machine (Type EKO; Erweka). The tablet thickness was 3.0–3.2 mm, and hardness was 6–8 kp.

2.3. Dissolution studies of the prepared kneaded powder complexes and tablets

For dissolution experiments, USP apparatus 2 (Model 85 T, Caleva Ltd.England) is used and operated at 75 rpm. In each flask, 300 mL of phosphate buffer (pH 6.8) was equilibrated to 37 °C ± 0.5 °C. Each of the prepared formulations (powder or tablet) was added to each flask. At specified time intervals for 6 h, samples were collected and their release runs performed in triplicate and absorbance measured at 244 nm. The amount of drug released was calculated as a cumulative percentage in relation to time.

Dissolution efficiency (DE) was calculated as follows:

$$DE = \frac{\int_1^2 ydt}{y_{100} \times (t_2 - t_1)} \times 100 \quad (3)$$

where, y is the percentage of dissolved product.

D.E. is the area under the dissolution curve between time points t_1 and t_2 expressed as a percentage of the curve at maximum dissolution, y100, over the same time period.

2.4. Permeation studies of the prepared kneaded powder complexes

For permeation experiments, each powder formulation was suspended in 5 mL of buffer within a cellophane membrane, tied and attached to the dissolution apparatus's paddle, and treated as in the dissolution experiments. A list of the prepared kneaded powder complexes and tablet formulae coding is shown in Table 2.

Table 1
FLB Tablet formulations.

Compossion	*F1*	*F2*	*F3*
FLB powder	25	–	–
Complex (1:1)	–	125	125
Carbopol	75	75	75
SLS	15	5	15
MCC	100	40	30
SSF	5	5	5

FLB: Flibanserin; SLS: sodium lauryl sulphate; MCC: microcrystalline cellulose; SSF: sodium sterayl fumarate.

2.4.1. Analysis of release data

According to the simplified Higuchi model, the mechanism of drug of each formulation (powder and tablet) was identified when the in vitro release data were fitted to different kinetic models, including zero-order, first-order, and diffusion-controlled release models, and assessed for the ability to describe the drug release pattern (Korsmeyer and Peppas, 1983).

Zero-order kinetic model:

$$C = C_o - -K_o t$$

where C is the drug concentration (released) at time t, C_o is the initial drug concentration, and K_o is the zero-order rate constant.

First-order kinetic model:

$$\log C = \log (C_o - -Kt)/2.303$$

where K = first-order rate constant.

Diffusion-controlled model:

$$Q_t = k_h t^{1/2}$$

where Q is the amount of drug released/unit area and K_h is Higuchi's release rate constant.

Korsmeyer—Peppas *model*:

$$Q_t/Q_\infty = kt^n$$

where Q_t/Q_∞ is the defined fraction of the released drug at a specified time t and n is the release exponent of the kinetic constant k. The release exponent n depends on the release mechanism; thus, it is used to characterize either the Fickian diffusion (n = 0.45) or the anomalous diffusion (non-Fickian transport) where ($0.45 < n < 0.89$); n = 0.89 indicates case II (relaxational) transport, and $n > 0.89$ indicates super-case II transport.

For permeation experiments, permeation parameters were determined on the basis of blotting the cumulative amount of the permeated drug ($\mu g.cm^{-2}.min^{-1}$) against time and then using the following equation:

$$P = J_{ss}/C_d$$

where P is the permeability coefficient (μg/cm), J_{ss} is the flux (slope of the linear line of the plot), and C_d is the concentration of the drug on the donor side.

2.4.2. Statistical analysis

GraphPad Prism software was used to analyze the data. In this regard, $p < 0.05$ indicated statistical significance.

3. Results and disscution

3.1. Spectrophotometric assay of FLB

The spectrophotometric scanning of FLB showed λmax at 244 nm (Fig. 1). The other excipients showed no interference at 244 nm. FLB was determined spectrophotometrically at λmax = 244 nm. A calibration curve was constructed. A linear relationship was observed between absorbance and the FLB concentration in phosphate buffer (pH 6.8) in a 25–400 μg/mL concentration range (Fig. 2). The regression equation is:

$y = 0.005x$, and thervalue was 0. 9999

Table 2
Sample coding for dissolution and permeation studies of FLB preparations.

Sample code	Discerption
B1 (Dissolution)	25 mg untreated FLB powder in buffer pH 6.8
B2 (Dissolution)	25 mg untreated FLB powder in buffer pH 6.8 contains 0.3% SLS
B3 (permeation)	25 mg untreated FLB powder in buffer pH 6.8
B4 (permeation)	25 mg untreated FLB powder in buffer pH 6.8 contains 0.1% SLS
B5 (permeation)	25 mg untreated FLB powder in buffer pH 6.8 contains 0.3% SLS
B6 (permeation)	25 mg untreated FLB powder in buffer pH 6.8 contains 0.5% SLS
C1 (Dissolution)	125 mg FLB kneaded complex in buffer pH 6.8
C2 (Dissolution)	125 mg FLB kneaded complex in buffer pH 6.8 contains 0.1 SLS
C3 (Dissolution)	125 mg FLB kneaded complex in buffer pH 6.8 contains 0.3 SLS
C4 (Dissolution)	125 mg FLB kneaded complex in buffer pH 6.8 contains 0.5 SLS
C5 (Permeation)	125 mg FLB kneaded complex in buffer pH 6.8
C6 (Permeation)	125 mg FLB kneaded complex in buffer pH 6.8 contains 0.1 SLS
C7 (Permeation)	125 mg FLB kneaded complex in buffer pH 6.8 contains 0.3 SLS
C8 (Permeation)	125 mg FLB kneaded complex in buffer pH 6.8 contains 0.5 SLS
C9 (permeation)	225 mg FLB kneaded complex (1:2) in buffer pH 6.8
C10(Dissolution)	225 mg FLB kneaded complex (1:2) in buffer pH 6.8
F1 (Dissolution)	Tablet from formula F1 in buffer pH 6.8
F2 (Dissolution)	Tablet from formula F2 in buffer pH 6.8
F3 (Dissolution)	Tablet from formula F3 in buffer pH 6.8

FLB: Flibanserin; SLS: sodium lauryl sulphate.

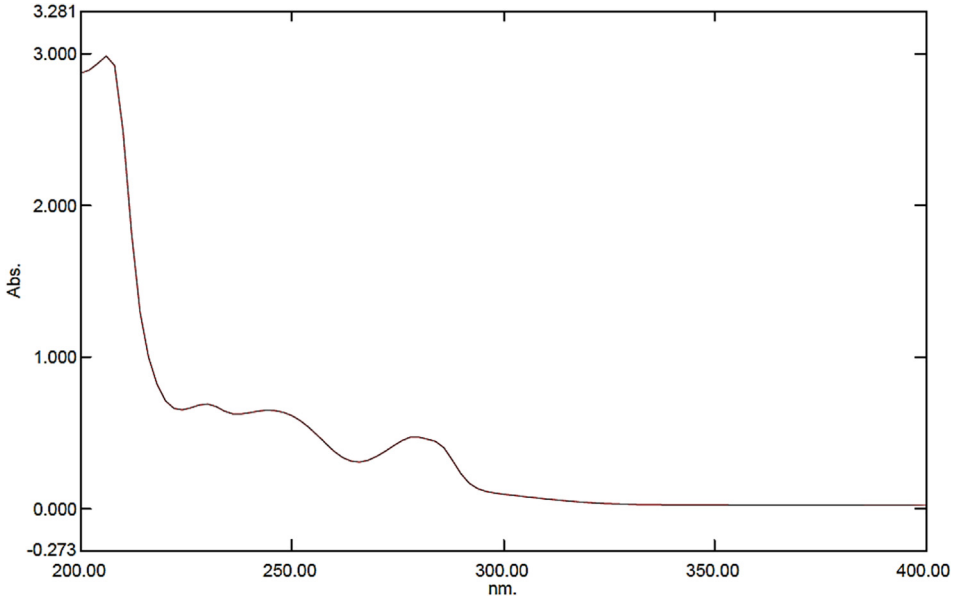

Fig. 1. Spectrophotometric scanning of FLB.

3.2. Phase solubility study

In most cases the main purpose of adding cyclodextrins to pharmaceutical products is to increase the aqueous solubility of poorly soluble drugs. The amount of cyclodextrin needed to obtain desired drug solubility is determined from a phase-solubility profile. Then the stability constant of the drug/cyclodextrin 1:1 complex is determined from Eq. (1) (Higuchi and Connors, 1965). For various reasons it is important to use as little cyclodextrin as possible in pharmaceutical preparations and, thus, the solubilizing efficiency of the cyclodextrins in the aqueous vehicle is the important aspect and not the absolute value of *K*1:1. The solubilizing efficiency is determined by either the slope of the phase-solubility profile (Eq. (2)) or the complex to free cyclodextrin concentration ratio, which is referred to as the complexation efficiency (CE) (Loftsson et al., 2005). On an average the reported CE value in literature is only about 0.3, meaning that on an average only about one out of every four cyclodextrin molecules in solution are forming a water-soluble complex with the poorly soluble drug, assuming 1:1 drug/-cyclodextrin complex formation. (Loftsson and Brewster, 2012)

The phase solubility profiles obtained for the HP-β-CD–FLB inclusion complexes are shown in Fig. 3. FLB aqueous solubility at zero HP-β-CD concentration (**S_0) was** 0.000467 **M.** The aqueous solubility of FLB linearly increased with the HP-β-CD concentration. The solubility diagram indicated the formation of a 1:1 HP-β-CD–FLB inclusion complex, as its shape showed a linear host–guest correlation (A_L type) and its slope was <1 (Chowdary and Srinivas, 2006). Obtained from the slope of the linear phase solubility diagram, K_c (the apparent stability constant) was found to be 372.54 M^{-1}. The greater Kc value the greater stability of the complex. Calculating CE value for HP-β-CD–FLB complex using Eq. (2) gave value of 0.21 indicating a moderate complexation efficiency.

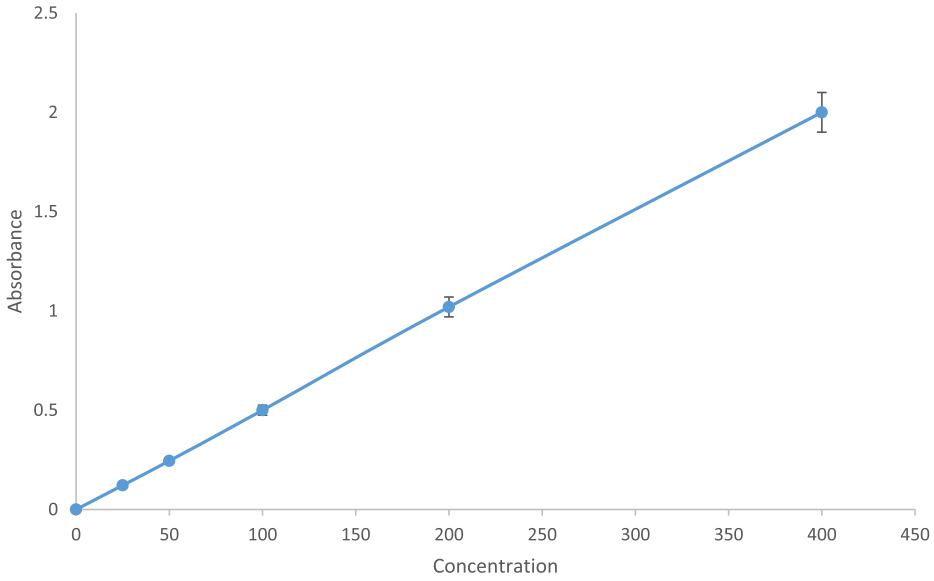

Fig. 2. Calibration curve of FLB.

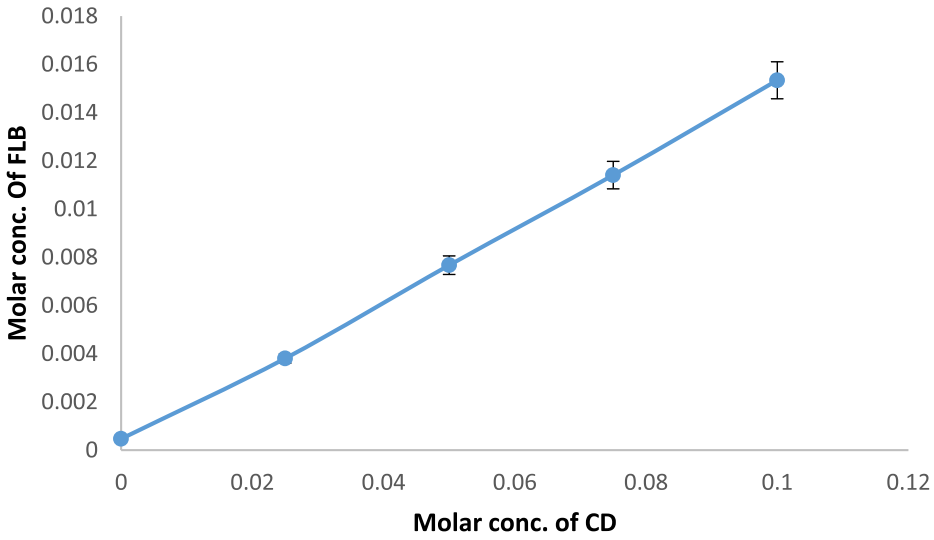

Fig. 3. Phase solubility curve.

3.3. Characterization studies

3.3.1. DSC and TGA studies

DSC was performed to examine the physical interactions between FLB and HP-β-CD. The DSC thermogram of pure FLB (Fig. 4a) exhibited a melting endotherm at 162.0 °C, while the thermogram of pure HP-β-CD (Fig. 4b) was a broad endotherm ranging from about 70 °C to 110 °C, which is due to the presence of water (Guinesi and Cavalheiro, 2006). The 1:1 physical mixture of FLB and HP-β-CD (Fig. 4c) displayed the same melting peak of FLB with the loss of its sharp peak due to a decrease in FLB and the presence of the CD carrier (dilution effect). The results obtained with the 1:1 HP-β-CD–FLB inclusion complex (Fig. 4d) demonstrated a marked decrease in the intensity of the FLB melting peak, which could indicate successful formation of the inclusion complex. For further confirmation of inclusion complex formation, TGA analysis was performed on abovementioned samples. TGA could help us check the thermal stability of pure FLB, HP-β-CD, physical mixture and the inclusion complex. Fig. 5 showed that the thermal weight loss process of HP-β-CD was started at 311 °C. The pure FLB began to lose weight, and a large weightlessness step appeared at 245 °C, the physical mixture began to lose weight, and a large weightlessness step appeared at 261 °C, The inclusion complex began to lose weight at 305 °C, and the rate of weight loss was relatively slow. The above results indicated that the inclusion complex had the stronger thermal stability than both of FLB or the physical mixture, which was related to the cavity matching between FLB molecule and HP-β-CD. Similar observations were previously reported for other drugs. (Sambasevam et al., 2013; Gao et al., 2019).

3.3.2. FTIR studies

In the IR spectrum of FLB (Fig. 6a), there were assigned peaks at 1686 and 1610 cm^{-1} and in the region of 1401–1448 cm^{-1}, reflecting, respectively, —C═O stretching, N—H bending, and aromatic C═C. Fig. 6b shows the FTIR spectrum of HP-β-CD in which O—H

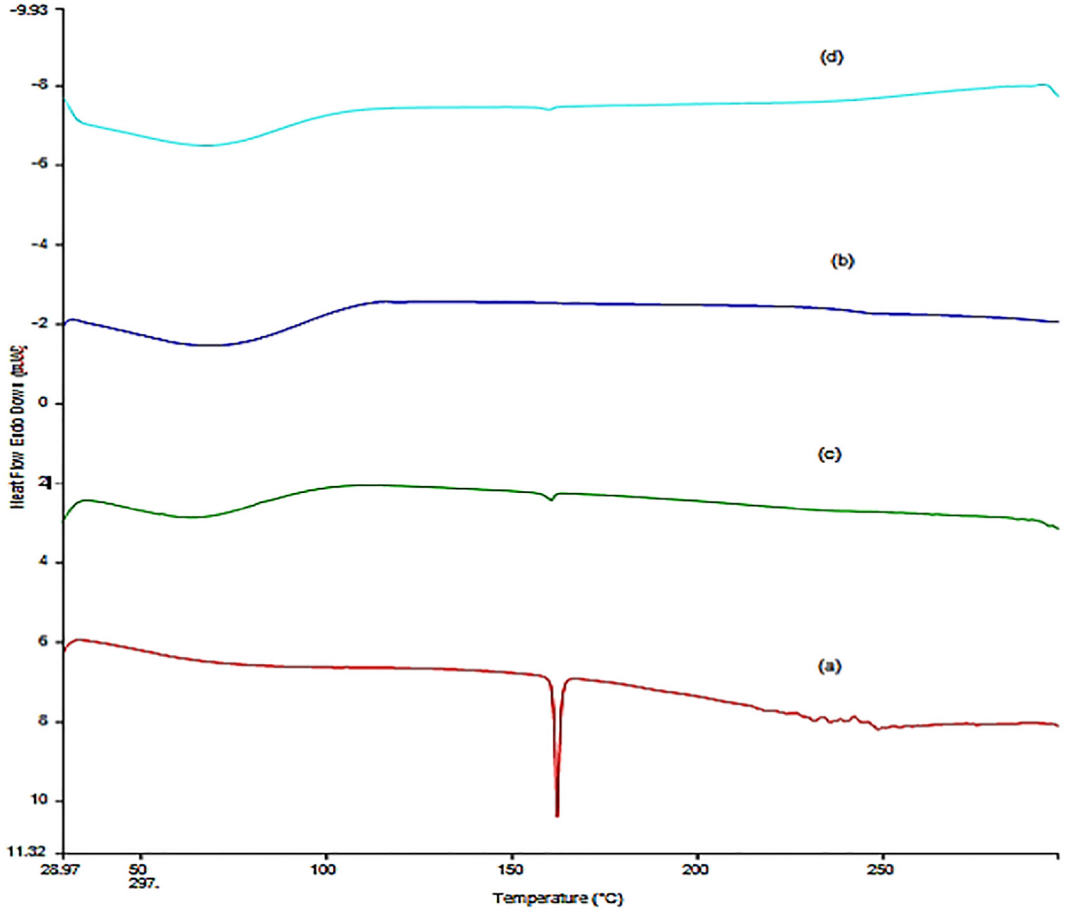

Fig. 4. DSC thermograms of FLB (a), HP-BCD (b), physical mixture (c), complex (d).

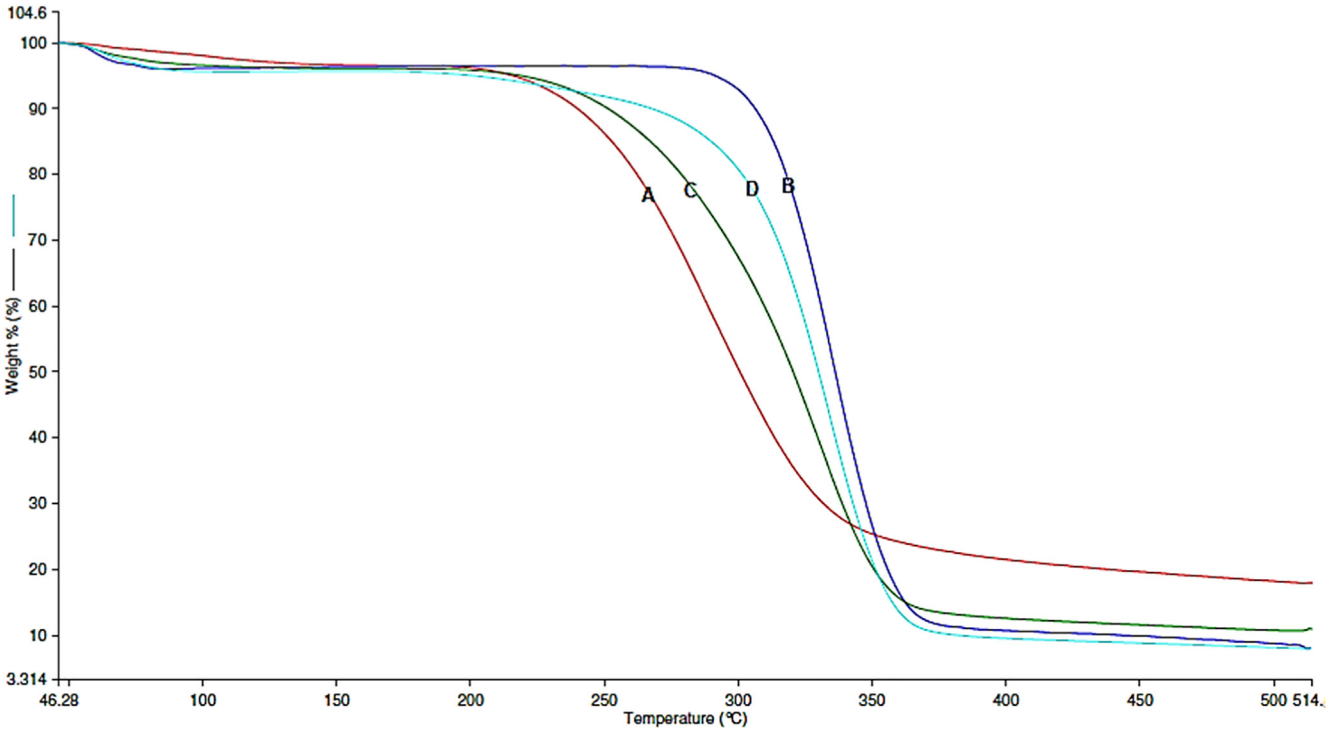

Fig. 5. TGA thermograms of FLB (a), HP-BCD (b), physical mixture (c), complex (d).

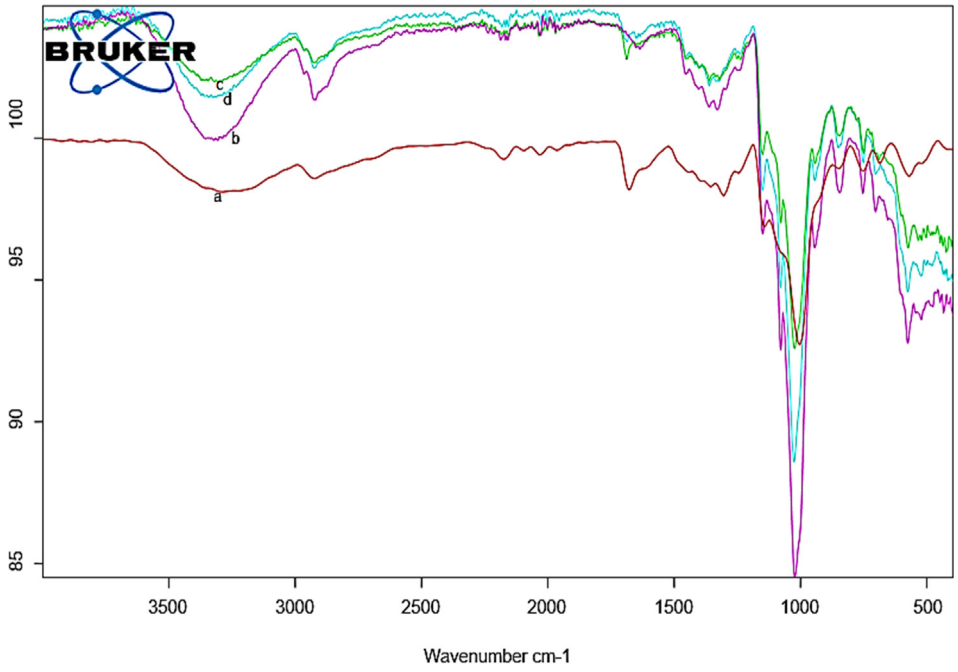

Fig. 6. FDIR of FLB (a), HP-BCD (b), physical mixture (c), complex (d).

stretching vibrations were assigned to a broad absorption band at 3423 cm^{-1}. For the C—H bond, there were intense peaks at 2931 cm^{-1} assigned to its stretching vibrations, while bands in the range of 1384–1460 cm^{-1} were assigned to the bending vibrations of CH_2 and CH_3. With regard to physical misture, the respective IR spectra demonstrated differential variations marked by decreased peak intensities in comparison to the IR spectra of pure FLB and CD (Fig. 6c). The bands' intensities between 1681 and 1306 cm^{-1}, assigned to the stretching vibrations of C═O and the bending from the aromatic ring of N—H, were comparably influenced by the formation of the complex with CD (Fig. 6d). In addition to these quantitative differences observed, there also were qualitative differences in the IR spectra of pure FLB and CD and the binary systems, specifically in the fingerprint regions where superimposition highlighted significant differences between the complex and individual pure compounds. These quantitative and qualitative differences between the IR spectra of pure compounds and the binary systems specifically the inclusion compound provide evidence of the interactions between the two compounds in the binary systems in this study. Similar observations were reported (Ahmed and Abdallah, 2020).

3.3.3. Powder X-ray diffractometry

Fig. 7 shows the XRD patterns of FLB and inclusion complexes prepared using kneading. FLB showed a crystalline pattern with characteristic peaks at 15.3°, 17.1, 19°, 20.2°, 26.4° and 50.2°. In contrast, HP-β-CD demonstrated an amorphous pattern. When physical trituration was used to prepare HP-β-CD–FLB inclusion complexes, XRD revealed crystalline peaks of FLB, indicating that physical trituration is not effective in preparing inclusion complexes with FLB. Some new diffraction peaks appeared in physical mixture at 38°, 44°, and 78. This may be due to the interaction of the un complexed drug with CD to form a new crystalline form (Li et al., 2016). However, the 1:1 HP-β-CD–FLB inclusion complex prepared using kneading revealed mostly an amorphous appearance, indicating the successful formation of an HP-β-CD–FLB inclusion complex using kneading.

3.4. Dissolution study forKneaded powder complexes and tablets

The release rate profile in the dissolution study was represented by the cumulative percent release on the *y* axis and time on the x axis. FLB as a weak base is more soluble in acidic medium. However, pH 6.8 was chosen in this study for dissolution and permeation experiments. The reason for that is to simulate the pH of buccal cavity.

Fig. 8 shows that the HP-β-CD–FLB inclusion complexes (C1 and C10) prepared using kneading (1:1 and 1:2) released about 46% ± 3.1% and up to 48% ± 3.2% of the drugs in 6 h, respectively. In contrast, 18% ± 0.5% of pure FLB was released in 6 h. It was evident that the HP-β-CD–FLB inclusion complexes showed a significantly faster dissolution rate than FLB alone ($p < 0.05$). However, the increased molar ratio led to an insignificant increase in drug release ($p > 0.05$). This could be probably due to the moderate calculated CE value (Loftsson et al., 2005).

In addition, the DE at 6 h for the HP-β-CD–FLB inclusion complexes increased by twofold (Table 3). There are several reasons that could contribute to the increased dissolution rate of FLB in the case of HP-β-CD–FLB inclusion complexes, including FLB amorphization and the formation of soluble inclusion complexes, leading to an increased dissolution rate, and better wettability.

3.4.1. Effect of SLS on dissolution

One approach to formulating poorly soluble drugs into solution is based on their solubilization in surfactant solutions above the critical micelle concentration (CMC). In this study, we used the anionic surfactant SLS (CMC = 8.3 mM, i.e., <0.1%) at different concentrations (0.1%, 0.3%, and 0.5%) to enhance the dissolution of FLB powder and HP-β-CD–FLB inclusion complexes. The results are shown in Table 3 and Fig. 9. The presence of SLS in the dissolution medium (0.3%) increased the dissolution rate of pure FLB. The DE at 6 h increased from 19.1% to 30.8%. For the 1:1M HP-β-CD–FLB inclusion complexes, the DE reached>80% within 30 min at all SLS concentrations used (Table3). A previous study showed significant improvement in the solubility of efavirenz by SLS, HP-β-CD, and polyvinylpyrrolidone (PVP K-30). Interestingly, the combina-

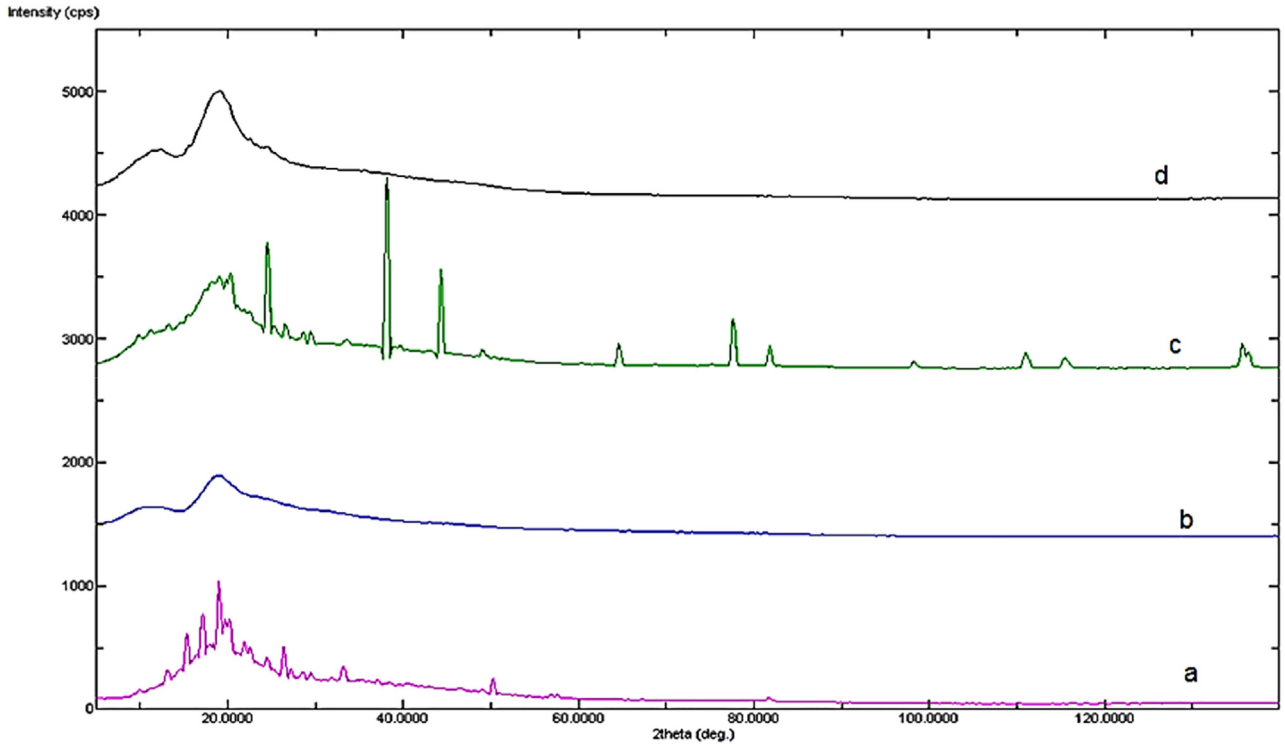

Fig. 7. Powder X-ray of FLB (a), HP-BCD (b), physical mixture (c), complex (d).

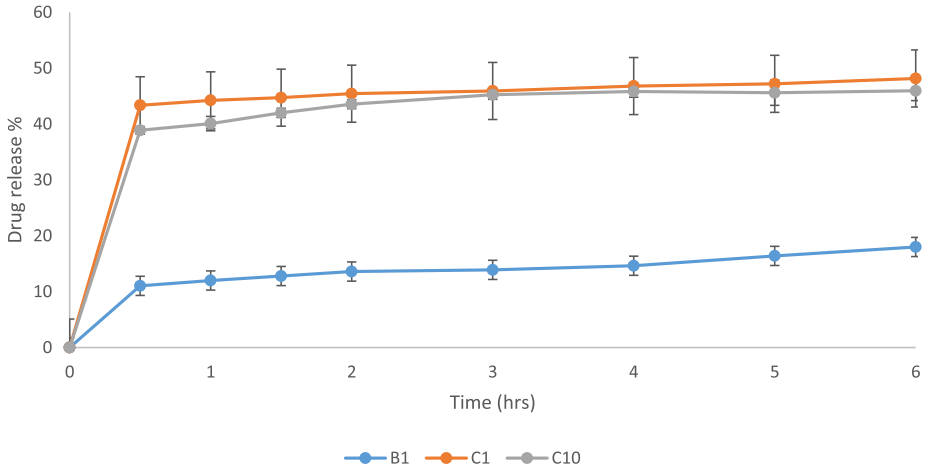

B1: 25mg untreated FLB powder

C1: 125mg FLB kneaded complex (1:1)

C10: 225mg FLB kneaded complex (1:2)

Fig. 8. Effect of complexation on FLB dissolution in buffer.

tion of HP-β-CD with SLS and PVP K-30 led to a notable enhancement in efavirenz's solubility in comparison to SLS and PVP K-30 alone (Chowdary and Naresh, 2011). In another study, both β-CD or SLS significantly increase the dissolution rate of celecoxib tablets (2.39- to 2.46-folds) (Chowdary and Gopichand, 2011).

As an application of the solubility study, bioadhesive buccal tablets were formulated (Table 1) and tested for drug release. Formula F1 which untreated FLB showed ~20% DE at 6 h. In the meantime, the dissolution rate of FLB from the kneaded systems was enhanced. Tablet formula F2 which contain FLB kneaded complex 1:1 and 5 mg of SLS, showed ~34% DE at 6 h. Furthermore, by increasing the amount of SLS to 15 mg/tablet (Formula F3), dissolution was significantly enhanced and the DE reached ~62% at 6 h, as shown in Table 3 and Fig. 10. Presenc of polymers in tablet formulae could also contribute in FLB release ehhancement. It was reported that presence of polymers could increase the CE and dissolution rate of CD complexes (Neto et al., 2018).

The kinetic parameters of the dissolution results are shown in Table 4. Formulas B1 and C1 showed an anomalous non-Fickian release pattern, while formula B2 nearly approached the Highchi

Table 3
Dissolution Efficiency of FLB formulae.

Formula	DE% (6 hrs.)
B1	19.1 ± 0.76
B2	30.83 ± 1.23
C1	38.6 ± 1.54
C2	81.3 ± 2.44
C3	83.5 ± 2.5
C4	85.6 ± 2.57
C10	39.4 ± 0.71
F1	20.29 ± 0.82
F2	34.15 ± 1.36
F3	61.85 ± 2.16

FLB: Flibanserin; DE: Dissolution Efficiency.

diffusion model. For tablet formulations, both F1 and F2 showed $n > 0.89$, indicating super-case II transport. Finally, formula F3 showed an anomalous non-Fickian release pattern, indicating a combination of diffusion and erosion mechanisms controlling FLB release.

3.5. Permeation studies through cellophane membrane

To assess the impact of different SLS concentrations in the dissolution medium on FLB permeation, the assessment of drug fluxes from the untreated powder and complexes via semipermeable cellophane membranes was performed. Complexing drug with CD is known to affect several physicochemical properties of the drug molecules, including chemical stability and aqueous solubility. In addition, this method enhances drug penetration in topical formulations (Loftssona and Jarvinen, 1999; Loftsson et al., 1999; Matsuda and Arima, 1999; Uekama et al., 1998). It is unclear how CDs enhance permeation, yet several mechanisms have been proposed (Loftsson and Olafsson, 1998). CDs are believed to work as hydrophilic carriers delivering hydrophobic drug molecules in an aqueous medium to the lipophilic membrane surface, where the drug molecules undergo partitioning from CDs to the membrane (Loftssona and Jarvinen, 1999). Interestingly, the large hydrophilic CD molecules remain within the aqueous medium as they have a low affinity for the lipophilic membrane. For instance, when 2- (HP-CD) was topically applied to the hairless mouse skin under occlusive conditions, only 0.02% of the dose was absorbed (Tanaka et al., 1995). Nevertheless, the drug flux via a biomembranes increases in direct correlation with the CD concentration in an aqueous solution with saturated drug levels. These observations are in line with the presence of an aqueous diffusion barrier on the membrane surface (Loftssona and Jarvinen, 1999; Loftsson et al., 1999). The approach of determining drug fluxes via semipermeable cellophane membranes has been adopted to assess the stability constants of drug–CD complexes and the drug release from CD-containing vehicles. Using membranes with a molecular weight cutoff above the molecular weight of CD, drug permeation from aqueous CD-containing vehicles via semipermeable cellophane membranes is comparable to that from lipophilic biomembranes (Loftssona and Jarvinen, 1999; Ono et al., 1999).

Fig. 11 shows the results of the permeation study of untreated FLB in release media with different SLS concentrations. Increasing the SLS concentration from 0.0% to 0.1% increased the of FLB flux. However, a further increase in the SLS concentration negatively affected FLB permeation. This result is in accordance with results reported in the literature for several cellophane membranes (Ghosh et al., 2011; Onyeji et al., 2009).

Fig. 12 and Fig. 13 show the effect of complexation on FLB permeation through the semipermeable cellophane membrane. The cumulative amount permeated at 6 h increased from 9.0% ± 0.49% for pure FLB to 14.16% ± 0.39% and 17.88% ± 0.127% for the 1:1 and 1:2 HP-β-CD–FLB inclusion complexes, respectively. An ex vivo permeability previous study (Altamimi et al., 2018), improved apparent permeability coefficient for the drug formulation containing β-CD when compared to the free drug was observed. Thus, confirming the observed improvements in the per-

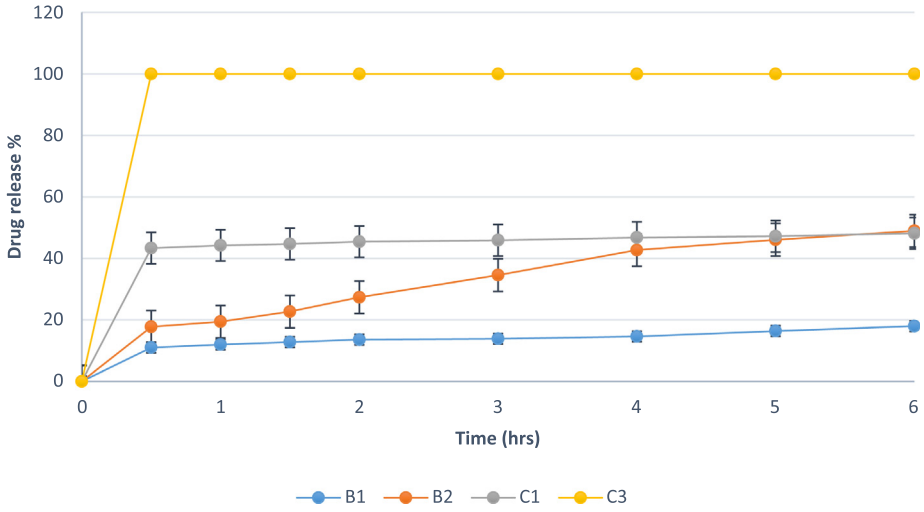

B1: 25mg untreated FLB powder in buffer pH 6.8

B2: 25mg untreated FLB powder in buffer pH 6.8 contains 0.3% SLS

C1: 125mg FLB kneaded complex in buffer pH 6.8

C3: 125mg FLB kneaded complex in buffer pH 6.8 contains 0.3 SLS

Fig. 9. Effect of SLS (0.3%) on dissolution of untreated and complexed FLB.

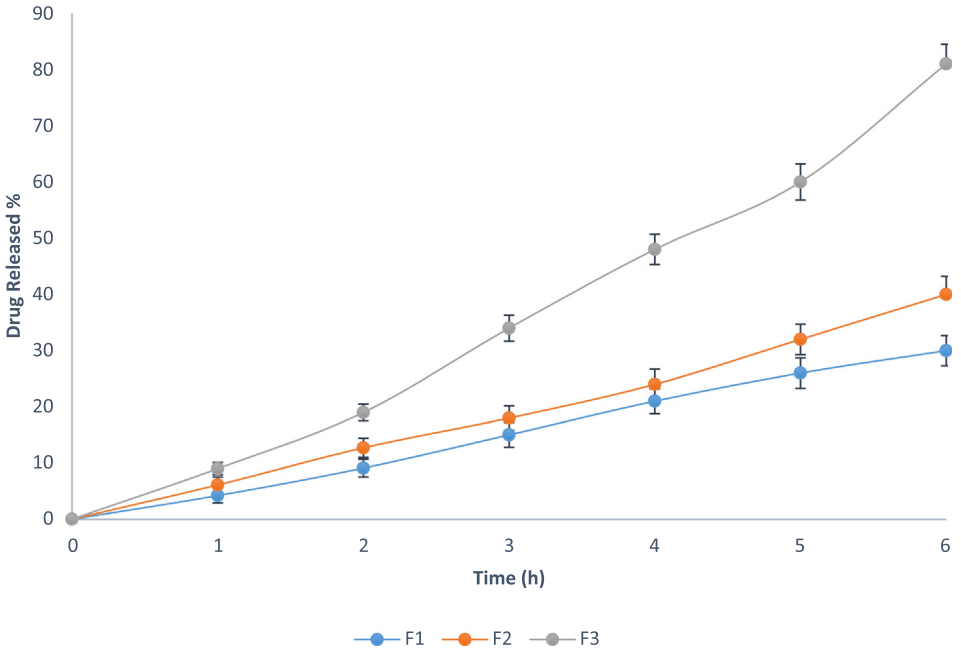

Fig. 10. FLB release from different tablet formulations.

Table 4
Kinetic Modeling of FLB Release from different preparations.

Release model		Sample code						
		B1	**C1**	**B2**	**C3**	**F1**	**F2**	**F3**
Zero order	R	0.767 ± 0.023	0.543 ± 0.016	0.955 ± 0.029	0.46 ± 0.014	0.991 ± 0.029	0.993 ± 0.03	0.941 ±0.028
	K_o (mg/min) $x10^{-3}$	8.2 ± 0.246	16.7 ± 0.501	30.3 ± 0.909	30.67 ± 0.92	29.68 ±0.89	55.41 ± 1.66	58.19 ±1.746
First order	R	0.783 ± 0.024	0.574 ±0.017	0.978 ±0.031	–	0.989 ± 0.0297	0.943 ± 0.028	0.921 ±0.0277
	K_1 (min^{-1}) $x10^{-5}$	6.95 ± 0.208	17.8 ±0.534	33 ± 0.99	–	28.66 ± 0.859	77.72 ± 2.331	193.23 ±5.77
Highchi diffusion model	R	0.908 ± 0.027	0.748 ±0.023	0.994 ± 0.029	0.68 ±0.021	0.943 ± 0.0283	0.923 ± 0.0277	0.998 ± 0.029
	K_h ($mg/min^{1/2}$)	0.2 ±0.006	0.47 ±0.014	0.65 ±0.02	0.93 ±0.028	0.582 ± 0.0175	1.06 ±0.0318	1.27 ±0.038
Log M/mas Vis log t	R	0.948 ± 0.028	0.982 ±0.03	0.996 ± 0.033	–	0.984 ±0.029	0.996 ±0.0309	0.977 ± 0.031
	n	0.18 ±0.006	0.037 ±0.001	0.425 ± 0.013	–	0.9711 ±0.0301	1.0492 ±0.0315	0.4039 ±0.0121
Selected model		anamoulas non-fickian release pattern		Higuchi diffusion model		Approaches Zero order		Higuchi diffusion model

Ko = zero-order rate constant, K_1 = first-order rate constant, K_h = Higuchi's release rate constant, R = correlation coefficients, n = the release exponent.

meability of HP-β-CD formulations developed in this study. The addition of SLS to the release medium showed a different pattern in comparison to its effect on dissolution. The cumulative amount permeated at 6 h increased significantly ($p < 0.05$) from 14.1% ± 0.39% to 21.88% and 34.56% by adding 0.1% and 0.3% SLS, respectively. However, increasing the SLS concentration to 0.5% did not increase FLB permeation. The results of permeation parameters are shown in Table 5. As reported in the literature, the semipermeable cellophane membrane, a weak cation exchanger, is anionic mainly due to the adsorption of anions present in the solution. The saturation and the strong interactions with the membrane matrix could be the reasons for obtaining low diffusion coefficients and permeability across the semipermeable cellophane membrane with 0.5% SLS solutions (Jain et al., 2004).

Biological membranes are generally lipophilic in nature, with an unstirred aqueous diffusion layer located at the outer membrane surface. β-CD is believed to enhance the permeation of drugs if permeation through the aqueous diffusion layer is the rate-limiting step in this process. As FLB and other class II drugs are characterized by their low aqueous solubility, the dissolution rate and permeation through the aqueous diffusion layer are limiting factors in oral absorption. However, class II drugs permeate biological membranes easily once in solution, achieving ≥90% absolute bioavailability. It was reported that β-CD increased the availability, partitioning, and, hence, permeability of hydrophobic drugs at the surface of the biological barrier without disrupting its structured lipid layers (Altamimi et al., 2018). Therefore, preparations of water-soluble HB-β-CD inclusion complexes of such drugs could increase diffusion and hence permeability through the mucosal surface.

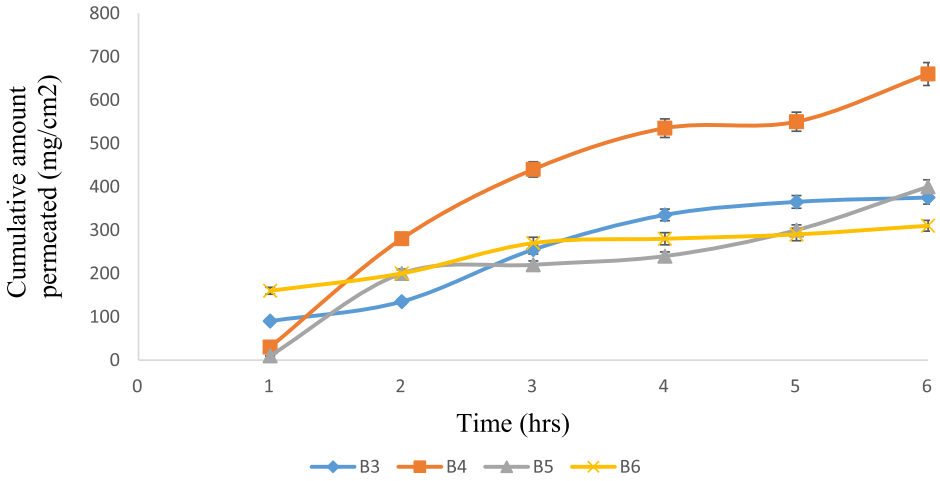

B3: 25mg untreated FLB powder in buffer pH 6.8

B4: 25mg untreated FLB powder in buffer pH 6.8 contains 0.1% SLS

B5: 25mg untreated FLB powder in buffer pH 6.8 contains 0.3% SLS

B6: 25mg untreated FLB powder in buffer pH 6.8 contains 0.5% SLS

Fig. 11. Effect of SLS on permeation of untreated FLB.

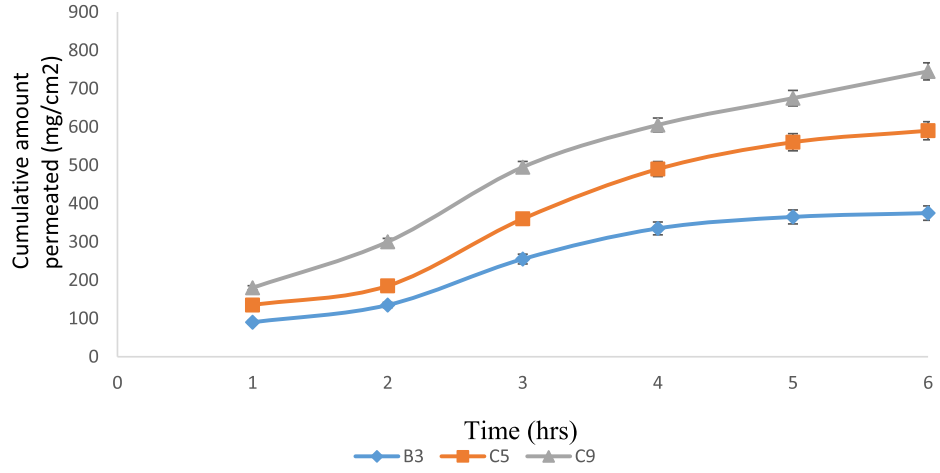

B3: 25mg untreated FLB powder

C5: 125mg FLB kneaded complex (1:1)

C9: 225mg FLB kneaded complex (1:2)

Fig. 12. Effect of complexation on FLB permeation in buffer.

4. Conclusion

HP-β-CD–FLB inclusion complexes were successfully prepared using the kneading method at 1:1 and 1:2 M ratios. Derived from the slope of the linear phase solubility diagram, the apparent stability constant $K_{1:1}$ was 372.54 M^{-1}. It was evident that the 1:1 HP-β-CD–FLB inclusion complex demonstrated an improved dissolution rate in comparison to FLB alone. Specifically, the DE at 6 h increased by twofold. The presence of SLS in the dissolution medium increased the dissolution rate of pure FLB and the HP-β-CD–FLB inclusion complex at all concentrations, with a more pronounced effect on the complex. The addition of SLS to the permeation medium showed enhanced permeation. The cumulative amount of FLB permeated from kneaded complexes1:1 at 6 h increased from 14.1% to 21.88% and 34.56% by adding 0.1% and 0.3% SLS, respectively.

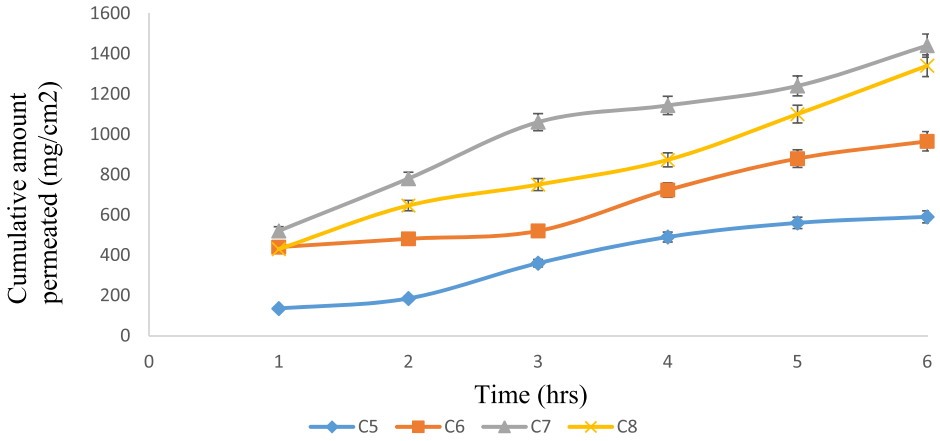

C5: 125mg FLB kneaded complex in buffer pH 6.8

C6: 125mg FLB kneaded complex in buffer pH 6.8 contains 0.1 SLS

C7: 125mg FLB kneaded complex in buffer pH 6.8 contains 0.3 SLS

C8: 125mg FLB kneaded complex in buffer pH 6.8 contains 0.5 SLS

Fig. 13. Effect of SLS on permeation of FLB complexes.

Table 5
Permeation parameters through cellophane membrane.

Sample code	Flux (Jss) ($\mu g/cm^2h^{-1}$)	Permeability coefficient (P) (μg /cm)
B3	62.7 ± 2.5084	0.0125
B4	115.88 ± 4.6352	0.0232
B5	64.85 ± 2.594	0.013
B6	33.07 ± 1.3228	0.0066
C5	100.85 ± 4.034	0.0202
C6	114.91 ± 4.2	0.0228
C7	173 ± 6.52	0.0346
C8	172 ± 6.88	0.0344
C9	116.1 ± 4.45	0.0232

Funding

The authors extend their appreciation to the Deanship of Scientific Research at King Saud University for funding this work through the research group project No. RG-1435-80.

Declaration of Competing Interest

The authors declare that they have no known competing financial interests or personal relationships that could have appeared to influence the work reported in this paper.

References

Ahmed, R.M., Abdallah, I.A., 2020. Determination of flibanserin in the presence of confirmed degradation products by a third derivative emission spectrofluorometric method: Application to pharmaceutical formulation. Spectrochim. Acta A Mol. Biomol. Spectrosc. 225, 117491.

Allers, K.A., Dremencov, E., Ceci, A., Flik, G., Ferger, B., Cremers, T.I., et al., 2010. Acute and repeated flibanserin administration in female rats modulates monoamines differentially across brain areas: a microdialysis study. J. Sex. Med. 7 (5), 1757–1767.

Altamimi, M.A., Elzayat, E.M., Alhowyan, A.A., Alshehri, S., Shakeel, F., 2018. Effect of beta-cyclodextrin and different surfactants on solubility, stability, and permeability of hydrochlorothiazide. J. Mol. Liq. 250, 323–328.

Carrier, R.L., Miller, L.A., Ahmed, I., 2007. The utility of cyclodextrins for enhancing oral bioavailability. J. Control. Release. 123 (2), 78–99.

Chowdary, K.P.R., Gopichand, G., 2011. Factorial study on the effects of beta-cyclodextrin and sodium lauryl sulphate on the solubility and dissolution rate of celecoxib tablets. Asian J. Chem. 23 (4), 1442–1444.

Chowdary, K.P.R., Naresh, A., 2011. A factorial study on the effects of HPβ-cyclodextrin, PVP K30 and SLS on the solubility and dissolution rate of Efavirenz. Int. J. Appl. Biol. Pharm. Technol. 2 (4), 228–234.

Chowdary, K.P.R., Srinivas, S.V., 2006. Effect of polyvinylpyrrolidone on complexation and dissolution rate of β- cyclodextrin and hydroxypropyl β-cyclodextrin complexes of celecoxib. Indian J. Pharm. Sci. 68, 631–634.

English, C., Muhleisen, A., Rey, J.A., 2017. Flibanserin (Addyi): The first FDA-approved treatment for female sexual interest/arousal disorder in premenopausal women. P T 42 (4), 237–241.

Fahmy, U.A., Ahmed, O.A.A., Badr-Eldin, S.M., Aldawsari, H.M., Okbazghi, S.Z., Awan, Z.A., et al., 2020. Optimized nanostructured lipid carriers integrated into in situ nasal gel for enhancing brain delivery of flibanserin. Int. J. Nanomed. 15, 5253–5264.

Gao, S., Bie, C., Ji, Q.Y., Ling, H.Y., Li, C.Y., Fu, Y., et al., 2019. Preparation and characterization of cyanazine-hydroxypropyl-beta-cyclodextrin inclusion complex. RSC Adv. 9 (45), 26109–26115.

George, S., Vasudevan, D., 2012. Studies on the preparation, characterization, and solubility of 2-HP-beta-cyclodextrin-meclizine HCl inclusion complexes. J. Young. Pharm. 4 (4), 220–227.

Ghosh, A., Biswas, S., Ghosh, T., 2011. Preparation and Evaluation of Silymarin beta-cyclodextrin molecular inclusion complexes. J. Young. Pharm. 3 (3), 205–210.

Guinesi, L.S., Cavalheiro, E.T.G., 2006. The use of DSC curves to determine the acetylation degree of chitin/chitosan samples. Thermochimica Acta. 444 (2), 128–133.

Higuchi, T., Connors, K., 1965. Phase-solubility techniques. Adv. Anal. Chem. Instrument. 4, 117–212.

Invernizzi, R.W., Sacchetti, G., Parini, S., Acconcia, S., Samanin, R., 2003. Flibanserin, a potential antidepressant drug, lowers 5-HT and raises dopamine and noradrenaline in the rat prefrontal cortex dialysate: role of 5-HT(1A) receptors. Br. J. Pharmacol. 139 (7), 1281–1288.

Jain, A., Ran, Y., Yalkowsky, S.H., 2004. Effect of pH-sodium lauryl sulfate combination on solubilization of PG-300995 (an anti-HIV agent): a technical note. Aaps. Pharmscitech. 5 (3).

Katz, M., DeRogatis, L.R., Ackerman, R., Hedges, P., Lesko, L., Garcia Jr., M., et al., 2013. Efficacy of flibanserin in women with hypoactive sexual desire disorder: results from the BEGONIA trial. J. Sex. Med. 10 (7), 1807–1815.

Korsmeyer, R.W., Peppas, N.A., 1983. Macromolecular and modeling aspects of swelling-controlled systems. Controlled Release Delivery Syst., 77–90

Li, J., Zhang, S., Zhou, Y., Guan, S., Zhang, L., 2016. Inclusion complexes of fluconazole with beta-cyclodextrin and 2-hydroxypropyl-beta-cyclodextrin in aqueous solution: preparation, characterization and a structural insight. J. Inclusion Phenomena Macrocyclic Chem. 84 (3–4), 209–217.

Loftsson, T., Brewster, M.E., 2012. Cyclodextrins as functional excipients: Methods to enhance complexation efficiency. J. Pharm. Sci. 101 (9), 3019–3032.

Loftsson, T., Hreinsdottir, D., Masson, M., 2005. Evaluation of cyclodextrin solubilization of drugs. Int. J. Pharm. 302 (1–2), 18–28.
Loftsson, T., Masson, M., Sigurjonsdottir, J.F., 1999. Methods to enhance the complexation efficiency of cyclodextrins. STP Pharma. Sci. 9 (3), 237–242.
Loftsson, T., Olafsson, J.H., 1998. Cyclodextrins: new drug delivery systems in dermatology. Int. J. Dermatol. 37 (4), 241–246.
Loftssona, T., Jarvinen, T., 1999. Cyclodextrins in ophthalmic drug delivery. Adv. Drug Deliv. Rev. 36 (1), 59–79.
Malaekeh-Nikouei, B., Nassirli, H., Davies, N., 2007. Enhancement of cyclosporine aqueous solubility using alpha- and hydroxypropyl beta-cyclodextrin mixtures. J. Incl. Phenom. Macrocycl. Chem. 59 (3–4), 245–250.
Matsuda, H., Arima, H., 1999. Cyclodextrins in transdermal and rectal delivery. Adv. Drug Deliv. Rev. 36 (1), 81–99.
Neto, A.C.D., da Rocha, A.B.D., Maraschin, M., Di Piero, R.M., Almenar, E., 2018. Factors affecting the entrapment efficiency of beta-cyclodextrins and their effects on the formation of inclusion complexes containing essential oils. Food Hydrocolloids 77, 509–523.
Ono, N., Hirayama, F., Arima, H., Uekama, K., 1999. Determination of stability constant of beta-cyclodextrin complexes using the membrane permeation technique and the permeation behavior of drug-competing agent-beta-cyclodextrin ternary systems. Eur. J. Pharm. Sci. 8 (2), 133–139.
Onyeji, C.O., Omoruyi, S.I., Oladimeji, F.A., Soyinka, J.O., 2009. Physicochemical characterization and dissolution properties of binary systems of pyrimethamine and 2-hydroxypropyl-beta-cyclodextrin. Afr. J. Biotechnol. 8 (8), 1651–1659.
Qiang, D.M., Gunn, J.A., Schultz, L., Li, Z.J., 2010. Evaluation of the impact of sodium lauryl sulfate source variability on solid oral dosage form development. Drug Dev. Ind. Pharm. 36 (12), 1486–1496.
Raj, R.A., Nair, S.S., Harindran, J., 2016. Formulation and Evaluation of Cyclodextrin Inclusion Complex Tablets of Carvedilol. Asian J. Pharma. 10 (2), 84–94.
Rasenack, N., Muller, B.W., 2005. Poorly water-soluble drugs for oral delivery - A challenge for pharmaceutical development - Part III: drug delivery systems containing the drug molecularly dispersed - Aspects on in vitro and in vivo characterization. Pharm. Ind. 67 (5), 583–591.
Sambasevam, K.P., Mohamad, S., Sarih, N.M., Ismail, N.A., 2013. Synthesis and Characterization of the Inclusion Complex of beta-cyclodextrin and Azomethine. Int. J. Mol. Sci. 14 (2), 3671–3682.
Tanaka, M., Iwata, Y., Kouzuki, Y., Taniguchi, K., Matsuda, H., Arima, H., Tsuchiya, S., 1995. Effect of 2-hydroxypropyl-beta-cyclodextrin on percutaneous absorption of methyl paraben. J. Pharm. Pharmacol. 47 (11), 897–900.
Uekama, K., Hirayama, F., Irie, T., 1998. Cyclodextrin drug carrier systems. Chem. Rev. 98 (5), 2045–2076.
Vikas, Y., Sandeep, K., Braham, D., Manjusha, C., Budhwar, V., 2018. Cyclodextrin complexes: an approach to improve the physicochemical properties of drugs and applications of cyclodextrin complexes. Asian J. Pharma. 12 (2), S394–S409.